

# A Phosphole Oxide-Containing Organogold(III) Complex for Solution-Processable Resistive Memory Devices with Ternary Memory Performances

Eugene Yau-Hin Hong, Chun-Ting Poon, and Vivian Wing-Wah Yam\*

Institute of Molecular Functional Materials [Areas of Excellence Scheme, University Grant Committee (Hong Kong)] and Department of Chemistry, The University of Hong Kong, Pokfulam Road, Hong Kong, P. R. China

**S** Supporting Information

**ABSTRACT:** A novel class of luminescent phosphole oxide-containing alkynylgold(III) complex has been synthesized, characterized, and applied as active material in the fabrication of solution-processable resistive memory devices. Incorporation of the phosphole oxide moiety in gold(III) system has been demonstrated to provide an extra charge-trapping site, giving rise to intriguing ternary memory performances with distinct and low switching threshold voltages, high OFF/ON1/ON2 current ratio of  $1/10^3/10^7$ , and long retention time for the three states. The present study offers vital insights for the future development of multilevel memory devices using small-molecule organometallic compounds.

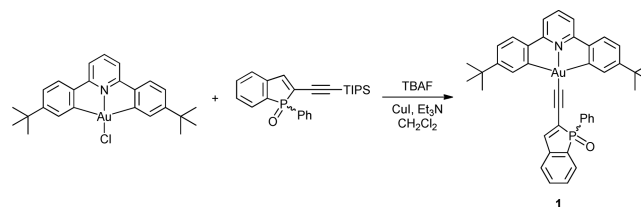
Innovative functional materials designed for organic memory devices have become highly desirable and aroused tremendous interest due to the rapid development of information technology;<sup>1–5</sup> in fact, conventional memory materials based on inorganic semiconductors have been facing various kinds of limitations, such as the growing demand for memory materials and the downscaling of cell size.<sup>1</sup> These have prompted the development of new materials for high-performance information storage, including metal oxides<sup>2</sup> and organic-based semiconducting materials,<sup>3</sup> of which the latter is of particular interest because of attractive features such as distinctive versatility, ease of fabrication, high flexibility, and low cost.<sup>3</sup> To date, the demand for advanced memory devices with high integration density for data storage is continuously increasing. However, existing organic memory devices are mostly binary systems based on electrical bistability, with the data storage capacity limited at  $2^n$ . One of the most effective measures to enhance the data storage capacity is by promoting the number of conductive states in memory devices to 3 or higher,<sup>4,5</sup> and interest in small-molecule-based multilevel memory materials has emerged very recently.<sup>5</sup>

Along with various small-molecule-based materials, organometallic complexes are potential contenders for offering alternative pathways in data storage thanks to their unique electronic features and luminescence properties. Compared to other transition metal complex systems, the family of gold(III) complexes is rather less explored and has recently gained increasing impetus for their versatile functional properties in various aspects, such as supramolecular assemblies<sup>6</sup> and phosphorescent emitters.<sup>7</sup> The interest in gold(III) complexes

also stems from their relatively high stability, environmental benignancy, and rich photoluminescence behavior,<sup>6a,7</sup> which together have made them ideal candidates for potential applications in optoelectronics. On the other hand, phosphole-containing  $\pi$ -conjugated systems are renowned for their distinctive nonplanar geometry at the phosphorus center,  $\sigma$ - $\pi$  hyperconjugation, and ease of functionalization.<sup>8</sup> In light of the promising structural diversity and fine-tuning opportunity, there have been continuous efforts toward the utilization of phosphole-based materials in electronic devices, such as organic light-emitting diodes (OLEDs)<sup>9</sup> and organic field-effect transistors (OFETs).<sup>10</sup> However, to the best of our knowledge, memory devices based on phosphole-containing materials have not yet been reported, despite their intrinsic electronic tunability and privileged electron-accepting properties due to hyperconjugation as well as the low-lying lowest unoccupied molecular orbital (LUMO).<sup>8</sup> In addition to the aforementioned scenarios together with our interest in organic memory devices<sup>5f,11</sup> and phosphole-based functional materials,<sup>12</sup> we hypothesized that, by judiciously incorporating phosphole oxide moieties into cyclometalated alkynylgold(III) systems and fine-tuning a delicate balance of their electronic properties, solution-processable organic memory devices with multilevel performance could be realized. Herein are presented a facile synthesis of the first phosphole oxide-containing gold(III) complex, its photophysical and electrochemical properties, and the results of studies of its promising ternary memory performances.

The target complex **1** was prepared in good yield through a one-pot synthesis by treating the chlorogold(III) precursor with 2-(triisopropylsilylethynyl)benzo[*b*]phosphole *P*-oxide in dichloromethane in the presence of tetra-*n*-butylammonium fluoride (TBAF), a catalytic amount of copper(I) iodide, and triethylamine (Scheme 1). The air-stable complex **1** was

**Scheme 1. Synthetic Pathway for Complex 1**



Received: March 11, 2016

Published: May 10, 2016

isolated as thermally stable solids with a decomposition temperature of ca. 292 °C, as determined by thermogravimetric analysis (Figure S1). It has been characterized by  $^1\text{H}$ ,  $^{31}\text{P}\{^1\text{H}\}$  NMR spectroscopy, FAB mass spectrometry, and elemental analysis. The molecular structure of **1** has also been confirmed by X-ray crystallography. The crystal structure determination data and selected bond lengths and angles are summarized in Tables S1 and S2, respectively. The perspective view of the crystal structure depicted in Figure 1 reveals a slightly distorted

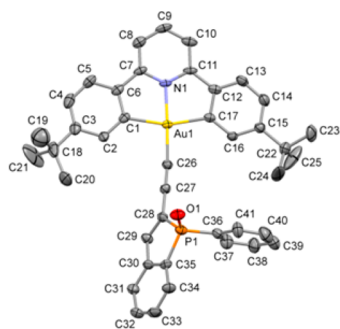


**Figure 1.** Perspective view of one enantiomer of **1** with atomic numbering scheme. Hydrogen atoms are omitted for clarity. Thermal ellipsoids are shown at the 30% probability level.

square planar geometry, in which the C(1)–Au(1)–C(17) and N(1)–Au(1)–C(26) bond angles are 162.1(2) and 177.4(2)°, respectively. The [Au( $^t\text{BuC}^{\wedge}\text{N}^{\wedge}\text{C}^t\text{Bu}$ )] motif is essentially coplanar, with Au(1)–C(1) and Au(1)–N(1) bond lengths of 2.087(6) and 2.011(4) Å, respectively. Such findings are comparable to those of related cyclometalated gold(III) complexes.<sup>7b–e</sup> Crystal packing of **1** (Figure S2) reveals that both enantiomers are present in the crystals selected for structure determination, and the complex molecules are partially stacked in a head-to-tail fashion with the shortest interplanar distance of ca. 3.5 Å, indicating the presence of weak  $\pi$ – $\pi$  stacking interactions in the solid state.

The alkynylgold(III) complex displays rich photophysical properties. The UV–vis absorption spectrum of **1** in dichloromethane at 298 K features an intense high-energy absorption at 290–325 nm, two moderately intense absorption bands at 350–390 nm, and a relatively weak absorption at 413 nm (Figure 2a). The photophysical data of complex **1** are summarized in Table S3. The low-energy absorption bands at 350–420 nm are assigned as derived predominantly from the metal-perturbed  $\pi$ – $\pi^*$  intraligand transitions of the  $^t\text{BuC}^{\wedge}\text{N}^{\wedge}\text{C}^t\text{Bu}$  tridentate ligand,<sup>7b–e</sup> with some mixing of the

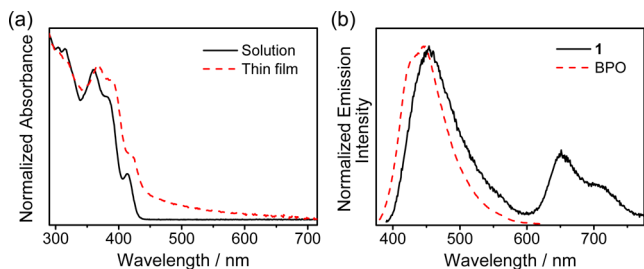


**Figure 2.** (a) UV–vis absorption spectra of **1** in dichloromethane solution and in the thin-film state. (b) Normalized emission spectra of **1** and 2-(triisopropylsilylethynyl)benzo[*b*]phosphole *P*-oxide (BPO) in degassed dichloromethane solution.

intraligand transitions of the benzophosphole oxide moiety (Figure S3). Compared with the absorption in solution state, the electronic absorption spectrum in thin film shows slight bathochromic shifts of ca. 7 nm (ca. 537  $\text{cm}^{-1}$  for the shift of the 361-nm band to 368 nm) in the absorption bands and an additional absorption tail (Figure 2a), indicative of the presence of weak  $\pi$ – $\pi$  stacking and an ordered packing of molecules in thin films. Interestingly, the alkynylgold(III) complex exhibits dual emissive behavior in degassed dichloromethane solution at 298 K (Figure 2b). Upon excitation at  $\lambda > 350$  nm, complex **1** displays a higher-energy band at 454 nm and a lower-energy vibronic-structured emission at 630–720 nm. The higher-energy band has an emission profile similar to that of the alkynyl ligand (Figure 2b), but with a slight bathochromic shift, and has been attributed to emission derived from the singlet metal-perturbed  $\pi$ – $\pi^*$  ligand-centered excited state of the benzophosphole oxide moiety. In contrast, the long-lived lower-energy emission shows relatively larger Stokes shift, indicating their triplet parentage. Thus, it is tentatively assigned as emission derived from the triplet excited state of metal-perturbed  $\pi$ – $\pi^*$  benzophosphole oxide ligand-centered origin.

The memory performances of the phosphole oxide-containing alkynylgold(III) complex have been studied by fabricating a memory device using **1**. Figure 3a illustrates a

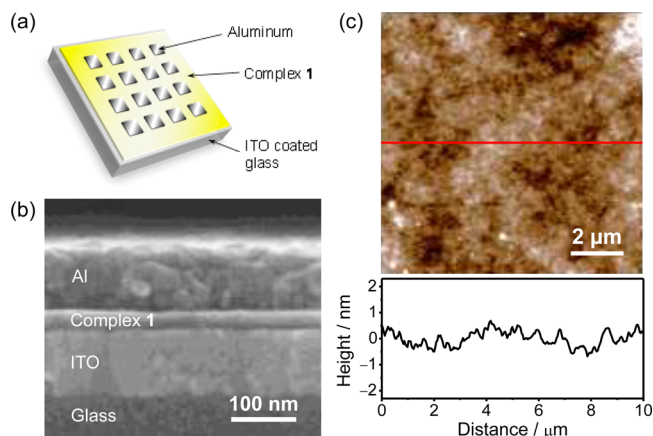


**Figure 3.** (a) Schematic diagram of the device structure. (b) SEM image of a cross-section of the device. (c) AFM topography and the corresponding height profile of the AFM topographic image.

schematic diagram of the memory device structure, in which a spin-coated layer of complex **1** is sandwiched between an indium–tin oxide (ITO) bottom electrode and a vacuum-deposited aluminum top electrode. The thickness of the complex film and aluminum has been determined to be ca. 30 and 100 nm, respectively, from the scanning electron microscopy (SEM) image of a cross-section of the device (Figure 3b). The surface morphology of the thin film formed from complex **1** has been studied by tapping mode atomic force microscopy (AFM). The AFM topography and the corresponding height profile depicted in Figure 3c indicate that the complex film possess a smooth surface with a root-mean-square roughness of ca.  $\pm 0.7$  nm. Such notable smoothness is believed to be a result of the weak  $\pi$ – $\pi$  stacking and ordered molecular packing in the thin film; a smooth interface is believed to be beneficial in governing an efficient charge transport and the resultant low threshold voltage.<sup>3g</sup>

The current–voltage ( $I$ – $V$ ) performance of the memory device fabricated with **1** is depicted in Figure 4a. In the first

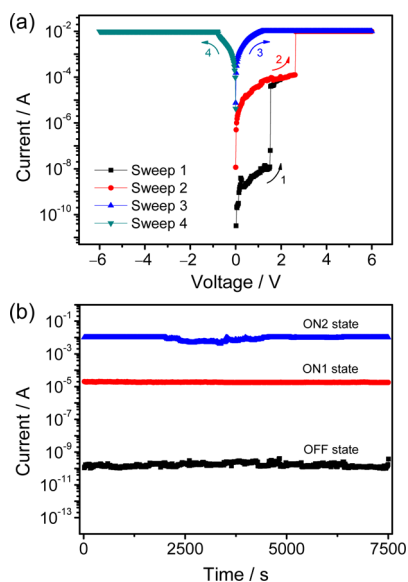


**Figure 4.** (a) Current–voltage characteristics of the memory device fabricated with complex **1**. (b) Stability of the device at different states under a constant voltage stress at 1 V.

sweep from 0 to 2 V, an abrupt increase in current has been observed at a switching threshold voltage ( $V_{Th1}$ ) of ca. 1.54 V, showing a transition from a low-conductivity (OFF) state to an intermediate-conductivity (ON1) state. The intermediate-conductivity (ON1) state can be maintained during the subsequent sweep, in which a transition from the intermediate-conductivity (ON1) state to a high-conductivity (ON2) state is also observed, revealing the presence of a second switching threshold voltage ( $V_{Th2}$ ) at ca. 2.64 V. The device remains in the ON2 state in the third sweep from 0 to 6 V, and the stability of the ON2 state is demonstrated by applying an inverse sweep from 0 to  $-6$  V. The ON2 state could be relaxed to the OFF state after switching off the power, showing a static random-access memory (SRAM) nature of the memory device.<sup>2b,3e,h</sup> The two discrete transitions in conductivity represent two “writing” processes of the memory device. These, together with a distinct current ratio of  $1:10^3:10^7$  for the three conductive states (OFF, ON1, ON2), indicate the ternary memory performance of the device. In addition, upon applying a constant stress of 1 V, there is no significant degradation in current for the three different states for more than 2 h (Figure 4b), suggesting a high durability of the memory performance and a low possibility of misreading errors. It is noteworthy that both threshold voltages are relatively low, which is desirable for low-power operation of memory devices.<sup>2b,3e,5b</sup> Consistent performance is also supported by the narrow distribution of the two threshold voltages and a constant voltage difference between them (Figure S4). To further verify the memory behavior, a device with a thicker complex layer (80 nm) has been fabricated (Figure S5). The device exhibits similar  $I$ – $V$  characteristics with ternary memory performances (Figure S6). Furthermore, it displays similar electrical switching under a negative bias (Figure S7), indicating that the alkyngold(III) complex-based device could work under both positive and negative voltage bias.

To provide further insights into the memory performance of complex **1**, its electrochemical properties have been studied by cyclic voltammetry. The cyclic voltammograms of **1** in dichloromethane (Figure 5a,b) show two quasi-reversible

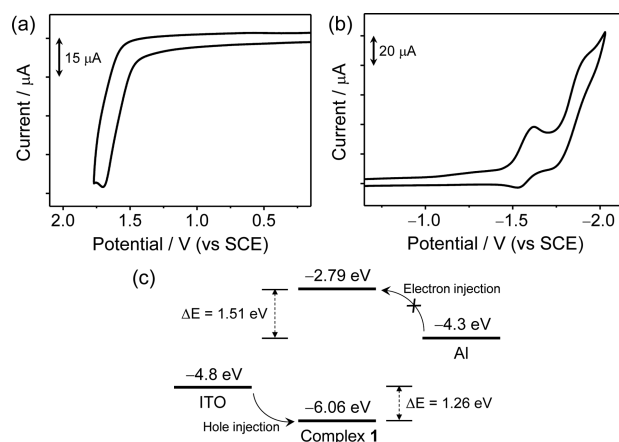


**Figure 5.** Cyclic voltammograms for the (a) oxidation and (b) reduction scans of complex **1** in dichloromethane (0.1 M  $\text{Bu}_4\text{NPF}_6$ ). Ferrocenium/ferrocene couple ( $\text{FeCp}_2^{+/0}$ ) was used as the internal reference for HOMO energy level. Scan rate =  $100 \text{ mV s}^{-1}$ . (c) Schematic diagram of the charge injection processes in the memory device.

reduction couples at  $-1.58$  ( $\Delta E = 75 \text{ mV}$ ) and  $-1.82 \text{ V}$  ( $\Delta E = 83 \text{ mV}$ ), and one irreversible oxidation wave at  $+1.73 \text{ V}$  vs saturated calomel electrode (SCE). The first and second reduction couples are assigned as the ligand-centered reductions of the  $^t\text{BuC}^{\wedge}\text{N}^{\wedge}\text{C}^t\text{Bu}$  ligand<sup>7d,e</sup> and the benzophosphole oxide alkyngyl ligand, respectively, while the oxidation wave is assigned as the alkyngyl ligand-centered oxidation. By using ferrocenium/ferrocene couple ( $\text{FeCp}_2^{+/0}$ ) as the internal reference, the energy levels of the HOMO and the LUMO are determined to be  $-6.06$  and  $-2.79 \text{ eV}$ , respectively, with an energy gap of  $3.27 \text{ eV}$ . The energy barrier between the work function of the ITO electrode ( $-4.8 \text{ eV}$ ) and the HOMO level is smaller than that between the work function of the aluminum electrode ( $-4.3 \text{ eV}$ ) and the LUMO level (Figure 5c), suggesting that the hole injection is energetically more favorable than the electron injection. The ternary memory behavior can be rationalized by the presence of two independent charge-trapping sites provided by the  $^t\text{BuC}^{\wedge}\text{N}^{\wedge}\text{C}^t\text{Bu}$  ligand and the benzophosphole oxide moiety, as revealed by cyclic voltammetry, which possess different electron-accepting abilities and would impede the mobility of the charge carriers in a stepwise manner. In comparison to our previous work on a binary memory device based on charge-transfer process of a donor–acceptor organogold(III) complex, which showed only one charge-trapping site,<sup>11a</sup> the present study demonstrates that a facile introduction of the electron-accepting benzophosphole oxide moiety into the cyclometalated gold(III) complex could alter the electrical switching mechanism and lead to a drastic tuning in the memory behavior, resulting in a promising ternary memory performance. It is envisaged that, with the intrinsic electron-accepting ability and privileged tunability of phosphole-containing compounds, as well as the unique optoelectronic properties of gold(III) complexes, high-performance memory devices with multilevel resistive states can be achieved.

To conclude, a new class of phosphole oxide-containing alkyngold(III) complex has been synthesized, structurally characterized, and applied in solution-processable resistive memory devices. High ternary memory performance has been demonstrated with distinct and low switching threshold voltages, high OFF/ON1/ON2 current ratio of  $1/10^3/10^7$ ,

and good stability of the three conductive states. The multilevel memory behavior has been attributed to the two independent charge-trapping sites provided by the cyclometalated ligand and the benzophosphole oxide moiety. The work presented herein provides guiding principles in designing novel functional organometallic compounds with multilevel memory effect. Further investigations on organic memories based on other phosphole-containing transition metal complexes and the fine-tuning of their memory performance are now in progress.

## ■ ASSOCIATED CONTENT

### ■ Supporting Information

The Supporting Information is available free of charge on the ACS Publications website at DOI: 10.1021/jacs.6b02629.

Experimental section; synthesis and characterization; thermogravimetric analysis; crystallographic data; photophysical data; distribution of threshold voltages; SEM image, and  $I$ - $V$  characteristics of the ITO/complex 1 (80 nm)/Al device (PDF)

X-ray crystallographic data for 1 (CIF)

## ■ AUTHOR INFORMATION

### Corresponding Author

\*wyyam@hku.hk

### Notes

The authors declare no competing financial interest.

## ■ ACKNOWLEDGMENTS

V.W.-W.Y. acknowledges support from The University of Hong Kong and the URC Strategic Research Theme on New Materials. This work has been supported by the French National Research Agency (ANR)/Research Grant Council (RGC) Joint Research Scheme (A-HKU704/12), the University Grants Committee Areas of Excellence Scheme (AoE/P-03/08), and the General Research Fund (GRF) Grant from the Research Grants Council of the Hong Kong Special Administrative Region, P. R. China (HKU 17305614). Dr. S. Y.-L. Leung is gratefully acknowledged for helpful discussions. We are grateful to Ms. Bella H. S. Chan from the Chinese University of Hong Kong for her assistance in X-ray crystal structure data collection and determination, and the Electron Microscope Unit at The University of Hong Kong for their technical assistance.

## ■ REFERENCES

- (1) (a) Kawata, S.; Kawata, Y. *Chem. Rev.* **2000**, *100*, 1777. (b) Raymo, M. F. *Adv. Mater.* **2002**, *14*, 401. (c) Wang, J. P. *Nat. Mater.* **2005**, *4*, 191.
- (2) (a) Waser, R.; Aono, M. *Nat. Mater.* **2007**, *6*, 833. (b) Waser, R.; Dittmann, R.; Staikov, G.; Szot, K. *Adv. Mater.* **2009**, *21*, 2632. (c) Yang, J. J.; Strukov, D. B.; Stewart, D. R. *Nat. Nanotechnol.* **2013**, *8*, 13.
- (3) (a) Möller, S.; Perlov, C.; Jackson, W.; Taussig, C.; Forrest, S. R. *Nature* **2003**, *426*, 166. (b) Ouyang, J.; Chu, C.-W.; Szmanda, C. R.; Ma, L.; Yang, Y. *Nat. Mater.* **2004**, *3*, 918. (c) Yang, Y.; Ouyang, J.; Ma, L.; Tseng, R. J.-H.; Chu, C.-W. *Adv. Funct. Mater.* **2006**, *16*, 1001. (d) Scott, J. C.; Bozano, L. D. *Adv. Mater.* **2007**, *19*, 1452. (e) Ling, Q.-D.; Liaw, D.-J.; Zhu, C.; Chan, D. S.-H.; Kang, E.-T.; Neoh, K.-G. *Prog. Polym. Sci.* **2008**, *33*, 917. (f) Cho, B.; Song, S.; Ji, Y.; Kim, T.-W.; Lee, T. *Adv. Funct. Mater.* **2011**, *21*, 2806. (g) Heremans, P.; Gelinck, G. H.; Müller, R.; Baeg, K.-J.; Kim, D.-Y.; Noh, Y.-Y. *Chem. Mater.* **2011**, *23*, 341. (h) Lin, W.-P.; Liu, S.-J.; Gong, T.; Zhao, Q.; Huang, W. *Adv. Mater.* **2014**, *26*, 570. (i) Li, G.; Zheng, K.; Wang, C.; Leck, K.

S.; Hu, F.; Sun, X. W.; Zhang, Q. *ACS Appl. Mater. Interfaces* **2013**, *5*, 6458. (j) Wang, C.; Wang, J.; Li, P.-Z.; Gao, J.; Tan, S. Y.; Xiong, W.-W.; Hu, B.; Lee, P. S.; Zhao, Y.; Zhang, Q. *Chem. - Asian J.* **2014**, *9*, 779. (k) Wang, C.; Gu, P.; Hu, B.; Zhang, Q. *J. Mater. Chem. C* **2015**, *3*, 10055.

(4) (a) Rozenberg, M. J.; Inoue, I. H.; Sanchez, M. J. *Phys. Rev. Lett.* **2004**, *92*, 178302. (b) Jung, Y.; Lee, S.-H.; Jennings, A. T.; Agarwal, R. *Nano Lett.* **2008**, *8*, 2056. (c) Liu, S.-J.; Wang, P.; Zhao, Q.; Yang, H.-Y.; Wong, J.; Sun, H.-B.; Dong, X.-C.; Lin, W.-P.; Huang, W. *Adv. Mater.* **2012**, *24*, 2901.

(5) (a) Li, H.; Xu, Q.; Li, N.; Sun, R.; Ge, J.; Lu, J.; Gu, H.; Yan, F. J. *Am. Chem. Soc.* **2010**, *132*, 5542. (b) Miao, S.; Li, H.; Xu, Q.; Li, Y.; Ji, S.; Li, N.; Wang, L.; Zheng, J.; Lu, J. *Adv. Mater.* **2012**, *24*, 6210. (c) Gu, P.-Y.; Zhou, F.; Gao, J.; Wang, C.; Xu, Q.-F.; Zhang, Q.; Lu, J.-M. *J. Am. Chem. Soc.* **2013**, *135*, 14086. (d) Li, Y.; Li, H.; Chen, H.; Wan, Y.; Li, N.; Xu, Q.; He, J.; Chen, D.; Wang, L.; Lu, J. *Adv. Funct. Mater.* **2015**, *25*, 4246. (e) Gu, Q.-F.; He, J.-H.; Chen, D.-Y.; Dong, H.-L.; Li, Y.-Y.; Li, H.; Xu, Q.-F.; Lu, J.-M. *Adv. Mater.* **2015**, *27*, 5968. (f) Poon, C.-T.; Wu, D.; Lam, W. H.; Yam, V. W.-W. *Angew. Chem., Int. Ed.* **2015**, *54*, 10569.

(6) (a) Yam, V. W.-W.; Au, V. K.-M.; Leung, S. Y.-L. *Chem. Rev.* **2015**, *115*, 7589. (b) Zhang, J.-J.; Lu, W.; Sun, R. W.-Y.; Che, C.-M. *Angew. Chem., Int. Ed.* **2012**, *51*, 4882. (c) Au, V. K.-M.; Zhu, N.; Yam, V. W.-W. *Inorg. Chem.* **2013**, *52*, 558. (d) Yim, K.-C.; Lam, E. S.-H.; Wong, K. M.-C.; Au, V. K.-M.; Ko, C.-C.; Lam, W. H.; Yam, V. W.-W. *Chem. - Eur. J.* **2014**, *20*, 9930.

(7) (a) Wong, K. M.-C.; Chan, M. M.-Y.; Yam, V. W.-W. *Adv. Mater.* **2014**, *26*, 5558. (b) Yam, V. W.-W.; Wong, K. M.-C.; Hung, L.-L.; Zhu, N. *Angew. Chem., Int. Ed.* **2005**, *44*, 3107. (c) Wong, K. M.-C.; Zhu, X.; Hung, L.-L.; Zhu, N.; Yam, V. W.-W.; Kwok, H. S. *Chem. Commun.* **2005**, 2906. (d) Wong, K. M.-C.; Hung, L.-L.; Lam, W. H.; Zhu, N.; Yam, V. W.-W. *J. Am. Chem. Soc.* **2007**, *129*, 4350. (e) Au, V. K.-M.; Wong, K. M.-C.; Tsang, D. P.-K.; Chan, M.-Y.; Zhu, N.; Yam, V. W.-W. *J. Am. Chem. Soc.* **2010**, *132*, 14273. (f) To, W.-P.; Tong, G. S.-M.; Lu, W.; Ma, C.; Liu, J.; Chow, A. L.-F.; Che, C.-M. *Angew. Chem., Int. Ed.* **2012**, *51*, 2654. (g) Tang, M.-C.; Tsang, D. P.-K.; Chan, M. M.-Y.; Wong, K. M.-C.; Yam, V. W.-W. *Angew. Chem., Int. Ed.* **2013**, *52*, 446. (h) Tang, M.-C.; Tsang, D. P.-K.; Wong, Y.-C.; Chan, M.-Y.; Wong, K. M.-C.; Yam, V. W.-W. *J. Am. Chem. Soc.* **2014**, *136*, 17861. (i) Cheng, G.; Chan, K. T.; To, W.-P.; Che, C.-M. *Adv. Mater.* **2014**, *26*, 2540.

(8) (a) Mathey, F. *Chem. Rev.* **1988**, *88*, 429. (b) Baumgartner, T.; Réau, R. *Chem. Rev.* **2006**, *106*, 4681. (c) Baumgartner, T. *Acc. Chem. Res.* **2014**, *47*, 1613.

(9) (a) Fave, C.; Cho, T.-Y.; Hissler, M.; Chen, C.-W.; Luh, T.-Y.; Wu, C.-C.; Réau, R. *J. Am. Chem. Soc.* **2003**, *125*, 9254. (b) Su, H.-C.; Fadhel, O.; Yang, C.-J.; Cho, T.-Y.; Fave, C.; Hissler, M.; Wu, C.-C.; Réau, R. *J. Am. Chem. Soc.* **2006**, *128*, 983. (c) Fadhel, O.; Gras, M.; Lemaître, N.; Deborde, V.; Hissler, M.; Geffroy, B.; Réau, R. *Adv. Mater.* **2009**, *21*, 1261.

(10) Matano, Y.; Saito, A.; Fukushima, T.; Tokudome, Y.; Suzuki, F.; Sakamaki, D.; Kaji, H.; Ito, A.; Tanaka, K.; Imahori, H. *Angew. Chem., Int. Ed.* **2011**, *50*, 8016.

(11) (a) Au, V. K.-M.; Wu, D.; Yam, V. W.-W. *J. Am. Chem. Soc.* **2015**, *137*, 4654. (b) Poon, C.-T.; Wu, D.; Yam, V. W.-W. *Angew. Chem., Int. Ed.* **2016**, *55*, 3647.

(12) (a) Chan, J. C.-H.; Lam, W. H.; Wong, H.-L.; Wong, W.-T.; Yam, V. W.-W. *Angew. Chem., Int. Ed.* **2013**, *52*, 11504. (b) Hong, E. Y.-H.; Wong, H.-L.; Yam, V. W.-W. *Chem. Commun.* **2014**, *50*, 13272.